

Linking Attention-Based Multiscale CNN With Dynamical GCN for Driving Fatigue Detection

Hongtao Wang[✉], Member, IEEE, Linfeng Xu[✉], Anastasios Bezerianos[✉], Senior Member, IEEE,
Chuangquan Chen[✉], Member, IEEE, and Zhiguo Zhang[✉], Member, IEEE

Abstract—Electroencephalography (EEG) signals have been proven to be one of the most predictive and reliable indicators for estimating driving fatigue state. However, how to make full use of EEG data for driving fatigue detection remains a challenge. Many existing methods include a time-consuming manual process or tedious parameter tunings for feature extraction, which is inconvenient to train and implement. On the other hand, most models ignore or manually determine EEG connectivity features between different channels, thus failing to thoroughly exploit the intrinsic interchannel relations for classification. In this article, we introduce a new attention-based multiscale convolutional neural network-dynamical graph convolutional network (AMCNN-DGCN) model, aiming to conquer these two issues in a unified end-to-end model. AMCNN-DGCN starts with attention-based multiscale temporal convolutions to automatically learn frequency filters to extract the salient pattern from raw EEG data. Subsequently, AMCNN-DGCN uses dynamical graph convolutional networks (DGCNs) to learn spatial filters, in which the adjacency matrix is adaptively determined in a data-driven way to exploit the intrinsic relationship between channels effectively. With the temporal-spatial structure, AMCNN-DGCN can capture highly discriminative features. To verify the effectiveness of AMCNN-DGCN, we conduct a simulated fatigue driving environment to collect EEG signals from 29 healthy subjects

Manuscript received October 12, 2020; revised November 23, 2020; accepted December 15, 2020. Date of publication December 25, 2020; date of current version January 15, 2021. This work was supported in part by the Special Projects in Key Fields Supported by the Technology Development Project of Guangdong Province under Grant 2020ZDZX3018, in part by the Special Fund for Science and Technology of Guangdong Province under Grant 2020182, in part by the Wuyi University and Hong Kong & Macao joint Research and Development Project under Grant 2019WGALH16, in part by the Science Foundation for Young Teachers of Wuyi University under Grant 2018td01, in part by the Jiangmen Brain-like Computation and Hybrid Intelligence Research and Development Center under Grant [2018]359 and Grant [2019]26, in part by the Scientific Research Startup Funds for High-Level Talents of Wuyi University under Grant 2020AL006, in part by the Guangdong Key Laboratory for Biomedical Measurements and Ultrasound Imaging under Grant SZD201909, in part by the Science, Technology and Innovation Commission of Shenzhen Municipality Technology Fund under Grant JCYJ20170818093322718, and in part by the National Natural Science Foundation of China under Grant 81871443. (*Hongtao Wang and Linfeng Xu contributed equally to this work.*) The Associate Editor coordinating the review process was Dr. Jing Lei. (*Corresponding authors: Chuangquan Chen, Zhiguo Zhang.*)

Hongtao Wang, Linfeng Xu, and Chuangquan Chen are with the Faculty of Intelligent Manufacturing, Wuyi University, Jiangmen 529020, China (e-mail: chenchuangquan87@163.com).

Anastasios Bezerianos is with the N1 Institute, National University of Singapore, Singapore 117456, and also with the Department of Medical Physics, University of Patras, 26500 Patras, Greece.

Zhiguo Zhang is with the Guangdong Key Laboratory for Biomedical Measurements and Ultrasound Imaging, Health Science Center, School of Biomedical Engineering, Shenzhen University, Shenzhen 518060, China (e-mail: zgzhang@szu.edu.cn).

Digital Object Identifier 10.1109/TIM.2020.3047502

(male/female = 17/12 and age = 23.28 ± 2.70 years) through a remote wireless cap with 24 channels. The results demonstrate that our proposed model outperforms six widely used competitive EEG models with high accuracy of 95.65%. Finally, the critical brain regions and connections for driving fatigue detection were investigated through the dynamically learned adjacency matrix.

Index Terms—Attention-based multiscale convolutional neural network (CNN), driving fatigue, dynamical graph convolution network (GCN), electroencephalography (EEG), spatiotemporal structure.

I. INTRODUCTION

DIVING fatigue degenerates a driver's control and judgment abilities, becoming one of the primary causes of fatal traffic accidents. Evidence has shown that driving fatigue accounts for 20%–30% of all vehicle accidents [1], which is a considerable threat to road safety. Due to these undesirable consequences, the measurement of driving fatigue state has attracted increasing attention in recent years. Among different indicators for measuring fatigue states, electroencephalography (EEG) can directly measure electrical activities originated from the brain, which contains rich information of human cognitive states and has been proven to be the most predictive and reliable one [2], [3].

In the past decades, many machine learning methods have been developed for EEG-based driving fatigue detection. Overall, existing methods usually consist of two steps: discriminative EEG feature extraction followed by supervised classification. Numerous kinds of feature extraction methods were developed for driving fatigue detection and achieved satisfactory performance. Regarding handcrafted features, frequency-domain features (such as power spectrum [4], [5] and entropy [6], [7]), and connectivity features [2] are predominantly used in driving fatigue detection. For frequency-domain feature extraction, the most common way is to extract features from each EEG signal channel independently in specific frequency bands, such as δ , θ , α , β , and γ bands. However, frequency-domain features neglect the spatial information of EEG signals and, thus, cannot reveal the interactions between multiple brain regions. The connectivity feature, on the contrary, can capture the spatial information through characterizing the interchannel relations. Commonly, the connectivity feature extraction method starts with a connectivity matrix (using existing methods, such as phase lag index (PLI) [8], phase-locked value (PLV) [9], and partial directional coherence (PDC) [10]) to quantify

the phase synchronization between electrode signals across multiple brain regions. Subsequently, a tedious manual process is adopted to calculate the desired features, such as strength, clustering coefficient, and eigenvector centrality of the connectivity matrix. It is widely acknowledged that the whole process of handcrafted feature extraction is tedious, time-consuming, and highly dependent on professional knowledge in the specific domain. Moreover, different scenarios of driving fatigue detection prefer various handcrafted features (e.g., power spectrum was adopted in [4] and [5], entropy was employed in [6] and [7], and connectivity feature was utilized in [2]). Although the convolutional neural network (CNN) can automatically extract the features from the raw EEG data, most of the existing works [11], [12] need to tune the kernel size through a grid search, which is time-consuming and inconvenient to train and implement.

On the other hand, regarding supervised classification for driving fatigue detection, existing studies have provided reliable and meaningful design solutions. In [13], the support vector machine (SVM) was trained with combined entropy features for automatic EEG detection of driving drowsiness. In our previous work [8], four types of classifiers, BP-Adaboost, random forest (RF), relevance vector machine (RVM), and SVM, were employed to evaluate the performances of connectivity features for driving fatigue detection. In [14], a novel complex network-based broad learning system was developed to assess EEG-based fatigue states. In [11], a novel channelwise CNN was developed to realize fatigue detection from raw EEG data. In [12], a new spatial-temporal CNN was introduced, which takes the inter-channel relations into account. CNN-based methods have shown competitive results for driving fatigue detection. However, typical CNN-based methods can only deal with the Euclidean structured data and restricts the model's input to grid data. Practically, existing CNN-based methods flatten EEG channels distributed on the 3-D irregular grid to a 2-D representation with a regular grid, which cannot adequately and accurately reflect the interaction between multichannel signals. Besides, most CNN-based methods only consider the relationships between the closest channels, which tends to lose some valuable information from distant channels. Since brain regions are located in a non-Euclidean space, the graph is the most appropriate data structure to represent brain connections. More specifically, each EEG channel is considered as a node of the graph, and the connection between channels is referred to as the edge of the graph. Recently, the graph convolution network (GCN) [15] under the graph theory was developed to cope with graph data. In [8], PLV-based GCN was proposed for multichannel EEG emotion recognition. In [16], PDC-based GCN was developed for driving fatigue detection. However, there are two issues with the existing GCN methods for driving fatigue detection. On the one hand, the adjacency matrix, which is a critical input of GCN describing the graph connection, must be determined in advance. The predetermined graph (such as PLI, PLV, and PDC) significantly affects the performance of the GCN. Due to the limited understanding of the complex brain, it is almost impossible to build a proper graph in advance for driving fatigue detection. On the

other hand, existing GCN models for driving fatigue detection are usually with handcrafted feature vectors [such as power spectral density (PSD) and differential entropy (DE)] as nodes in the graph. As a result, the model cannot be trained end-to-end, which tends to lose some valuable information and, thus, yield suboptimal results.

In this article, we introduce a new attention-based multiscale CNN-dynamical graph convolutional network (AMCNN-DGCN) model, aiming to conquer all the abovementioned issues in feature extraction and supervised classification. AMCNN-DGCN is a unified end-to-end framework, which simultaneously learns the discriminative EEG feature representations, classifies the driving fatigue states, and exploits the functional topological relationship of electrodes. The AMCNN-DGCN model starts with attention-based multiscale temporal convolutions to learn frequency filters from the raw EEG data, in which the kernel size is simply determined by the sampling rate of data, and hence, the tuning of kernel size is not necessary. Subsequently, the AMCNN-DGCN model uses dynamical GCN (DGCN) to learn spatial filters, in which the adjacency matrix is adaptively learned in a data-driven way, exploiting the intrinsic relationship between channels effectively. AMCNN-DGCN is with the temporal-spatial structure to extract more discriminative features and the compact model to alleviate overfitting problems, and thus, it can produce competitive results.

We elaborately design a driving fatigue experiment to acquire EEG data to verify the proposed AMCNN-DGCN model. Experimental results demonstrate that the proposed AMCNN-DGCN model is superior to the state-of-the-art models. We also investigate the critical brain regions and connections for driving fatigue detection. Our study showed that the frontal area and occipital area provide the most valuable information for driving fatigue detection, and the frontal-frontal and frontal-occipital connections are most informative.

The remainder of this article is organized as follows. Section II presents the proposed AMCNN-DGCN model with implementation details. Section III introduces the fatigue experiment, the acquisition and preprocessing of EEG signals, and the definition of alert states and the fatigue states according to the behavioral performance. Section IV provides the results compared with existing competitive models, followed by the ablation studies and analysis of the critical brain regions and connections. Finally, a conclusion is drawn in Section V.

II. METHOD

In this section, we first detail the framework of the proposed AMCNN-DGCN in Section II-A. Then, the algorithm of AMCNN-DGCN is present in Section II-B. Finally, Section II-C gives the implementation details for AMCNN-DGCN.

A. Model Architecture

As shown in Fig. 1, we introduce the AMCNN-DGCN model, end-to-end architecture for driving fatigue detection, based on the temporal-spatial structure of the EEG signals. The AMCNN-DGCN model orderly consists of three blocks:

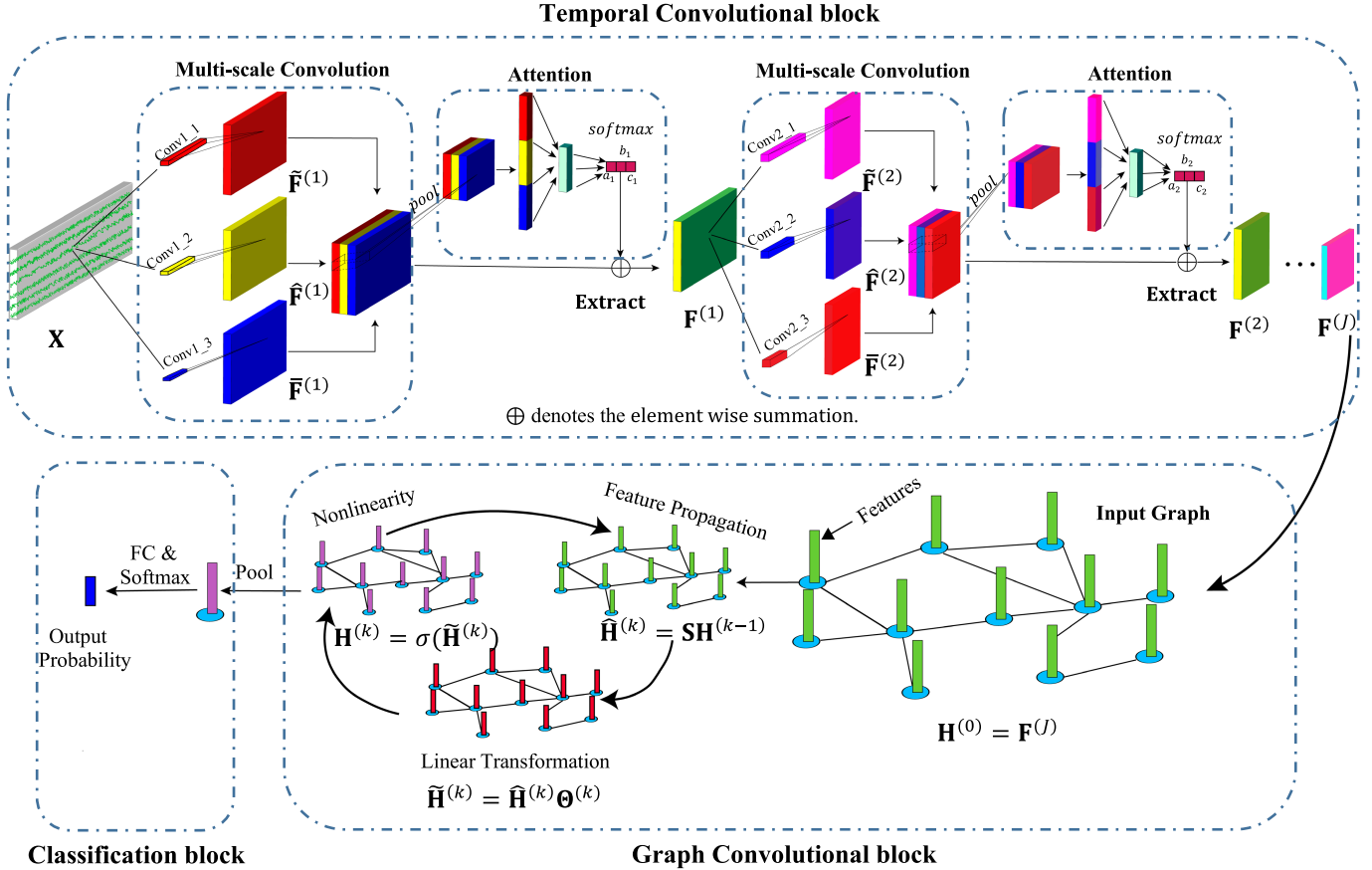


Fig. 1. Overall architecture of the AMCNN-DGCN model, which consists of three blocks: temporal convolutional block, graph convolutional block, and classification block. The input of the model is the EEG signals with n channels. The output is the predicted labels with probability.

temporal convolutional block, graph convolutional block, and classification block. We present the concrete model architecture in the following.

1) *Temporal Convolutional Block*: In the temporal convolutional block, we transform the signal in the time domain to learn frequency. A new feature representation for each channel is learned over multiple temporal convolution blocks. To guarantee the temporal convolution block can capture the salient signal accurately, it is critically important to determine the size of the kernel. Instead of tuning the kernel size, filters with different kernel sizes are employed to automatically capture temporal features over multiple time scales, followed by an attention layer to adaptively extract the salient pattern from multiple learned features. As illustrated in Fig. 1, the feature map with the j th temporal convolution block is denoted as $\mathbf{F}^{(j)} \in R^{n \times p_j}$, which consists of three operators: multiscale convolution, attention, and extract.

Multiscale Convolution: Suppose that we are given an EEG trail $\mathbf{X} = [\mathbf{x}_1, \dots, \mathbf{x}_n] \in R^{n \times T}$, $\mathbf{x}_n \in R^T$, having n channels and T sampling points in each channel. In the j th temporal convolution block, we first perform three transformations $\mathcal{F}_1 : \mathbf{X} \rightarrow \tilde{\mathbf{F}}^{(j)} \in R^{n \times p_j}$, $\mathcal{F}_2 : \mathbf{X} \rightarrow \hat{\mathbf{F}}^{(j)} \in R^{n \times p_j}$, and $\mathcal{F}_3 : \mathbf{X} \rightarrow \bar{\mathbf{F}}^{(j)} \in R^{n \times p_j}$ via a set of 1-D kernels with three different scales, i.e., low-scale, mid-scale, and high-scale. Batch normalization and ReLU activation functions are then applied sequentially to accelerate the learning process and improve performance.

Attention: We integrate the information from all the three branches $\tilde{\mathbf{F}}^{(j)}$, $\hat{\mathbf{F}}^{(j)}$, and $\bar{\mathbf{F}}^{(j)}$ to perform the attention operators. In detail, a pooling layer is first conducted independently on every branch to reduce the dimensionality of representations for better efficiency and avoid overfitting. These learned branches are flattened to a 1-D vector and concatenated together. Then, two fully connected layers and a softmax layer are applied in sequence to obtain normalized attention weights for the three convolution kernels.

Extract: We achieve the final feature map $\mathbf{F}^{(j)}$ by multiplying the attention weights with the learned representations of the three branches to extract the salient pattern

$$\mathbf{F}^{(j)} = a_j \tilde{\mathbf{F}}^{(j)} + b_j \hat{\mathbf{F}}^{(j)} + c_j \bar{\mathbf{F}}^{(j)}, a_j + b_j + c_j = 1. \quad (1)$$

Through incorporating features in different time scales, the temporal convolution block has a better generalization over different subjects and time-series tasks.

2) *Graph Convolutional Block*: In the graph convolutional block, we perform graph convolutional networks to learn spatial filters [17], [18]. In graph convolutional block, each EEG channel is considered as a node of the graph, and the connection between channels is referred to as an edge of the graph. We denote the graph as $G = (\mathbf{V}; \mathbf{A})$, in which $\mathbf{V} = \{v_1, v_2, \dots, v_n\}$ represents the vertex set with n nodes, and $\mathbf{A} = (a_{ij})_{n \times n}$ is a symmetric adjacency matrix describing the edge weight between nodes in \mathbf{V} . Each node v_i is with a

feature vector $f_i^{(J)} \in R^{p_j}$ learned after J temporal convolution blocks, and the feature matrix for all nodes is denoted as $\mathbf{F}^{(J)} = [f_1^{(J)}, \dots, f_n^{(J)}]^T \in R^{n \times p_j}$, where $f_i^{(J)}$ are concatenated as rows.

In the graph convolutional block, a new feature representation for each node is learned over multiple layers. In each graph convolution layer, three operations are employed to update the feature representation for each node, including feature propagation, feature transformation, and nonlinear transition [17]. The initial node representation $\mathbf{H}^{(0)}$ is the learned feature matrix extracted from the temporal convolutional block, i.e., $\mathbf{H}^{(0)} = \mathbf{F}^{(J)}$. The processing with the k th graph convolution layer is written as

$$\mathbf{H}^{(k)} = \sigma(\mathbf{SH}^{(k-1)}\Theta^{(k)}) \quad (2)$$

where $\mathbf{H}^{(k-1)}$ is the input node representations for all nodes in the k th graph convolution layer and $\mathbf{H}^{(k)} = [\mathbf{h}_1^{(k)}, \mathbf{h}_2^{(k)}, \dots, \mathbf{h}_n^{(k)}]^T$ is the output node representations. \mathbf{S} denotes the “normalized” adjacency matrix estimated by $\mathbf{S} = \mathbf{D}^{-(1/2)}\mathbf{AD}^{-(1/2)}$, where $\mathbf{D} = \text{diag}(d_1, d_2, \dots, d_n)$ is the diagonal degree matrix of \mathbf{A} , i.e., $d_i = \sum_j a_{ij}$, and $\Theta^{(k)} \in R^{d_{k-1} \times d_k}$ is a layer-specific trainable weight matrix.

The operation $\hat{\mathbf{H}}^{(k)} = \mathbf{SH}^{(k-1)}$ averages the feature vectors of neighbors around nodes, which is known as “feature propagation.” The feature \mathbf{h}_i of each node v_i is calculated by

$$\mathbf{h}_i^{(k)} = \frac{a_{ii}}{d_i + 1}\mathbf{h}_i^{(k-1)} + \sum_{j=1}^n \frac{a_{ij}}{\sqrt{(d_i + 1)(d_j + 1)}}\mathbf{h}_j^{(k-1)}. \quad (3)$$

The operation $\tilde{\mathbf{H}}^{(k)} = \hat{\mathbf{H}}^{(k)}\Theta^{(k)}$ is referred to as “feature transformation,” which transforms the smoothed hidden feature representations linearly. The operation $\mathbf{H}^{(k)} = \sigma(\tilde{\mathbf{H}}^{(k)})$ corresponds to a “nonlinear transition,” in which a nonlinear activation function was applied pointwise to $\tilde{\mathbf{H}}^{(k)}$.

3) *Classification Block:* In the classification block, the features are passed to a dense layer for feature aggregation and then a softmax layer for classification. After K graph convolution layers, the class prediction for \mathbf{X} is expressed as

$$\hat{\mathbf{y}} = \text{softmax}(\text{pool}(\mathbf{H}^{(K)})\mathbf{W}) \quad (4)$$

where $\hat{\mathbf{y}} \in R^C$ is the predicted label with C class, $\text{pool}(\cdot)$ applies pooling over the nodes in the graph, $\mathbf{W} \in R^{d_K \times C}$ denotes the weights connecting the DGCN layer and the output layer, and the softmax layer serves as a normalizer across all classes. Sum pooling is adopted in our model because it has shown more expressive power than max pooling and mean pooling [19].

B. Algorithm for AMCNN-DGCN Model

Suppose that we are given N labeled training data set $\{\mathcal{X}, \mathcal{Y}\} = \{\mathbf{X}_i, \mathbf{y}_i\}_{i=1}^N$, where $\mathcal{X} \in R^{N \times n \times d}$, $\mathcal{Y} \in R^{N \times C}$, and $\mathbf{y}_i \in \{0, 1\}^C$. In the AMCNN-GCN model, \mathbf{X}_i is first transformed to $\mathbf{F}^{(J)}$ using the temporal convolutional block based on (1), then is changed to $\mathbf{H}_i^{(K)}$ using the graph convolutional block based on (2), and, finally, produces a predicted label $\hat{\mathbf{y}}_i$ based on (4).

The adjacency matrix $\mathbf{A} \in R^{n \times n}$, with n channels in the AMCNN-DGCN model, plays an important role in graph representation learning. In the AMCNN-DGCN model, the adjacency matrix \mathbf{A} characterizes the interchannel relationship, which is learnable instead of being statically predetermined [15]. Specifically, the AMCNN-DGCN model starts with randomly initialized connections between channels and then iteratively updates the connections according to the loss function.

We adopted cross-entropy loss to evaluate the inconsistency between the true label \mathbf{y}_i and the predicted label $\hat{\mathbf{y}}_i$. To simultaneously learn the optimal adjacency matrix, the loss function is written as

$$L = \frac{1}{N} \sum_{i=1}^N \text{cross_entropy}(\hat{\mathbf{y}}_i, \mathbf{y}_i) + \alpha \|\Theta\| + \beta \|\mathbf{A}\|_1 \quad (5)$$

where Θ denotes all the trainable model parameters, and $\|\cdot\|_1$ represents the l_1 -norm. The terms $\alpha \|\Theta\|$ and $\beta \|\mathbf{A}\|_1$ are used for regularization. With the l_1 sparse regularization to assess the sparse graphic representation, the critical connections between channels can be simultaneously obtained. The training stage of the AMCNN-DGCN model is detailed in Algorithm 1.

Algorithm 1 AMCNN-DGCN Model (Training Stage)

Input: A labeled data set $\{\mathcal{X}, \mathcal{Y}\} = \{\mathbf{X}_i, \mathbf{y}_i\}_{i=1}^N$, number of epochs T_1 , number of batches in each epoch T_2 , other regularization hyper-parameters

Output: The learned adjacency matrix \mathbf{A} and the model parameter Θ for the AMCNN-DGCN model.

Initialize the model parameters Θ in AMCNN-DGCN model
Randomly Initialize the adjacency matrix \mathbf{A}

```

for  $t_1 = 1: T_1$  do
    for  $t_2 = 1: T_2$  do
        Sample one batch size of samples  $\mathbf{X}_{\text{batch}}$  and  $\mathbf{y}_{\text{batch}}$  from  $\mathcal{X}$  and  $\mathcal{Y}$ , respectively
        Calculate the learned feature map  $\mathbf{F}_{\text{batch}}^{(J)}$  by passing  $\mathbf{X}_{\text{batch}}$  into the temporal convolution block based on Eq. (1)
        Calculate the output node representations  $\mathbf{H}_{\text{batch}}^{(K)}$  by passing  $\mathbf{F}_{\text{batch}}^{(J)}$  into the graph convolution block based on Eq. (2)
        Calculate the prediction label  $\hat{\mathbf{y}}_{\text{batch}}$  by passing  $\mathbf{H}_{\text{batch}}^{(K)}$  into the classification block based on Eq. (4)
        Use  $\mathbf{y}_{\text{batch}}$  and  $\hat{\mathbf{y}}_{\text{batch}}$  to calculate the loss function based on Eq. (5)
        Update the adjacency matrix  $\mathbf{A}$  and the model parameters  $\Theta$  via Adam optimizer according to the loss function
        end for
    end for

```

C. Implementation Details for AMCNN-DGCN Model

We aim to design a compact architecture for AMCNN-DGCN that: 1) can alleviate overfitting problems and 2) can exhibit a better efficiency. Therefore, the number of temporal convolutional blocks and the number of graph convolutional blocks are only selected from 1 to 4.

TABLE I
AMCNN-DGCN ARCHITECTURE

| Block | Layer | Kernel size | stride | Input | Output | Activation |
|----------------------|-----------------|--------------------------|--------|------------------------|------------------------|------------|
| Temporal convolution | Input | | | | (n,T,1) | |
| | Conv1_1 | (1, T//q) | 2 | | | ReLU |
| | Conv1_2 | (1, T//2q) | 2 | (n,T,1) | (n, p ₁ ,3) | ReLU |
| | Conv1_3 | (1, T//4q) | 2 | | | ReLU |
| | Attention1 | | | (n, p ₁ ,3) | (n, p ₁ ,1) | softmax |
| | Conv2_1 | (1, p ₁ //q) | 2 | | | ReLU |
| | Conv2_2 | (1, p ₁ //2q) | 2 | (n, p ₁ ,1) | (n, p ₂ ,3) | ReLU |
| | Conv2_3 | (1, p ₁ //4q) | 2 | | | ReLU |
| | Attention2 | | | (n, p ₂ ,3) | (n,p ₂ ,1) | softmax |
| | Reshape | | | (n, p ₂ ,1) | (n,p ₂) | |
| Graph convolution | GCN1 | | | (n, p ₂) | (n, d ₁) | ReLU |
| | GCN2 | | | (n, d ₁) | (n, d ₂) | ReLU |
| | GCN3 | | | (n, d ₂) | (n, d ₃) | ReLU |
| Classifier | Global_add_pool | | | (n, d ₃) | d ₃ | |
| | FC | | | d ₃ | C | softmax |

where n is the number of channels, T is the number of sampling points, and C is the number of classes. To reduce the tunable hyperparameters, the kernel sizes are simply chosen to be $1/q$, $1/2q$, $1/4q$ of the sampling points of the data, respectively. $p_1 = \lceil \frac{T-T//4q}{2} \rceil + 1$, $p_2 = \lceil \frac{p_1-p_1//4q}{2} \rceil + 1$, and the dimension of nodes in each graph convolution layer is simply set as follows: $d_2 = d_1/2$ and $d_3 = d_2/2$. We set $q = 5$ and $d_1 = 200$ according to a small amount of trial-and-error (q is selected from 4 to 6, and d_1 is selected from 100 to 400 by the step size of 100).

Through a small amount of trial-and-error, we observed that AMCNN-DGCN achieves superior accuracy under two temporal convolutional blocks (i.e., $J = 2$) and three graph convolutional blocks (i.e., $K = 3$). A description of the AMCNN-DGCN model can be found in Table I.

In the process of training initialization, the Xavier normal distribution is adopted to initialize the weight of the network. The model is fitted using Adam optimizer with the learning rate 0.0001 and other default parameters, as described in [20]. The regularization terms α and β in (5) are equally set to 0.02. We train the model with PyTorch on a workstation equipped with an Intel CPU (i7-9700k, 3 GHz) and an NVIDIA GPU (RTX 2080 Ti). To comprehensively evaluate the model, we use fivefold cross-validation to obtain the model with the highest accuracy. On average, it takes 380 epochs to train the network, and the training time is about 34 min.

III. EXPERIMENT

A. Subjects

The EEG acquisition experiments were conducted at the Cognitive Engineering Laboratory, Centre for Life Sciences, National University of Singapore (NUS), Singapore; 29 healthy students (male/female = 17/12 and age = 23.28 ± 2.70 years) without any mental disorders were recruited and performed the experiments. We ensured that all the subjects met the following inclusion criteria for two days before the experiment: 1) no intake of antifatigue drinks and drowsiness-causing medications and 2) enough sleep with over 7 h per night. All the subjects were required to be familiar with the system to eliminate operational errors before the

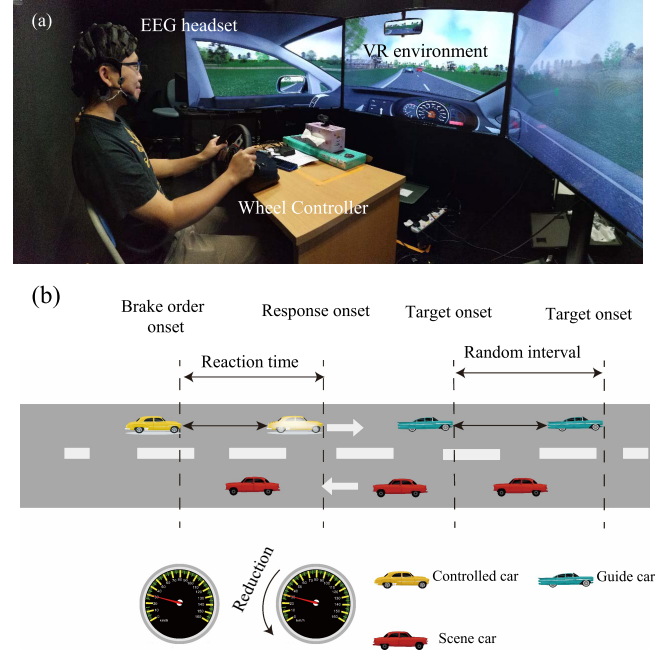


Fig. 2. (a) Experimental scenario of the experiment. (b) Subjects drive the controlled car (yellow) on a two-way rural road and randomly receive a brake signal elicited from the guide vehicle (blue). Reaction time corresponds to the interval between the brake order onset generated from the guide car (blue) and the response onset performed by the subject. The speed of the controlled car was recorded throughout the experiment.

experiment. This study received written informed consent from all subjects and was approved by the Institutional Review Board of NUS.

B. Experimental Protocol

Referring to Fig. 2, the simulated driving environment includes a simulated driving system and a wearable wireless dry-sensor EEG acquisition system. Specifically, we equip the simulated driving system with a Logitech G27 Racing Wheelset for car operation, a three-65-in-LCD-screen display to show a panorama of road condition, and a host computer to provide the driving environment. Subjects were required to follow Singapore's traffic regulations and drive the car on a two-way rural road for one and a half hours. The subject (driving the yellow car) randomly received the brake signal generated from a (blue) guide car and was asked to take a corresponding brake to keep a safe distance. We used the reaction time of the subject and the speed variation of the vehicle to quantitatively assess the subject's behavioral performance. Reaction time records the latency between the brake order elicited from the guide car and the subsequent brake operation performed by the subject. More details about the simulated driving experiment can be referred to our previous study [21].

C. Data Acquisition and Preprocessing

To make the driving fatigue detection more convenient and comfortable, we collected the EEG signals by Cognionics headset (model: HD-72, Cognionics Inc., USA) with 24 electrodes at a sampling frequency of 250 Hz [see Fig. 3(a)]. All the electrodes were arranged in accordance with the International 10/20 system, and the electrode impedance was maintained below 20 k Ω throughout the recordings.

The acquired data were further filtered into 1–40 Hz by a bandpass filter and rereferenced against the common average reference (CAR). Subsequently, the widely used independent component analysis (ICA) was applied to remove the artifact components [22]. We conducted the preprocessing algorithms using EEGLAB [23] with the in-house MATLAB scripts.

According to statistical analysis of behavioral performance in terms of reaction time and speed variation [see Fig. 3(b)], we define the first 10-min blocks and last 10-min blocks as the alert states and the fatigue states, respectively. We selected EEG data within these two blocks (20 min in total) to verify the proposed model. Then, the signals were divided into a series of 1-s samples without any overlap, resulting in 1200 samples per subject (20 min = 1200 s).

IV. RESULT

In this section, the effectiveness of the proposed model is evaluated on the data set described in Section III. Specifically, we first access the overall performance of the proposed AMCNN-DGCN model through fivefold cross-validation. Then, the AMCNN-DGCN model is further compared with six widely used competitive EEG models to further explore the benefits of the proposed model. We also conduct ablation studies to assess the impact of every component of our AMCNN-DGCN model. Finally, the critical brain regions and connections for driving fatigue detection were investigated through the dynamically learned adjacency matrix.

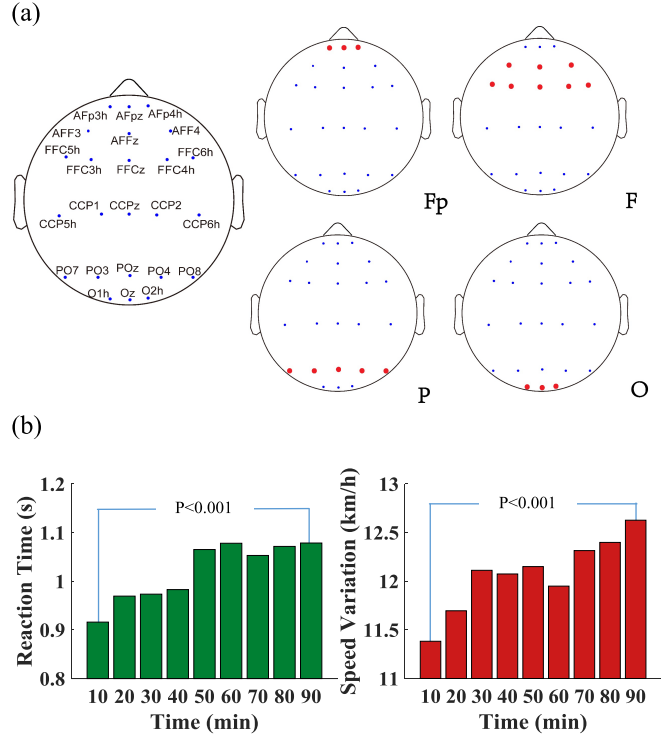


Fig. 3. Scalp used for the experiment and statistical analysis of behavioral performance. (a) Distribution of the employed electrodes and the subdivision of the EEG channels according to their locations: Fp: frontal pole; F: frontal; P: parietal; and O: occipital. (b) Reaction time and speed variation in 10-min bin during the experiment.

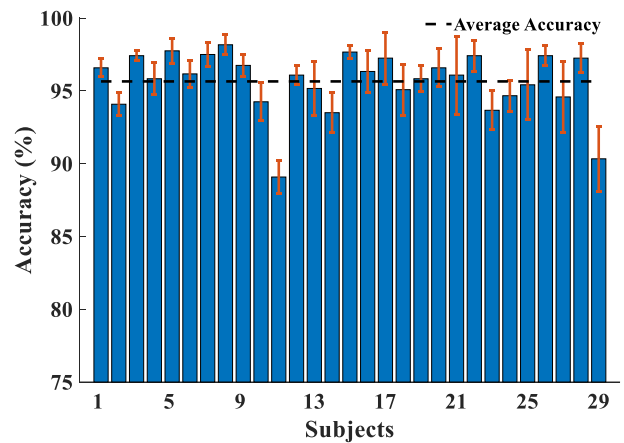


Fig. 4. Overall performance of the AMCNN-GCN model.

A. Overall Performance

The proposed AMCNN-DGCN model was trained by fivefold cross-validation to obtain the individual performances on 29 subjects. As seen from Fig. 4, the proposed AMCNN-DGCN model performs well on the entire data set, and the lowest accuracy is found at 89.08% in Sub#11. The differences in accuracy may be due to the subject's physical conditions. By examining the experiment's recorded video, we found that sub#11 stayed alert in the first 75-min blocks and only showed slight fatigue in the last 15-min blocks. As a result, it may be difficult to distinguish the fatigue of sub#11 from the collected EEG data. The AMCNN-DGCN

model achieves an average accuracy of 95.65% with a standard deviation of 2.10%, and the accuracies of 18 subjects surpass the average accuracy. These results demonstrate that the proposed AMCNN-DGCN model is effective and stable for driving fatigue detection. The encouraging performance of the AMCNN-DGCN model can be attributed to two factors: 1) a spatial-temporal structure to extract more discriminative features and 2) a compact model to alleviate the overfitting problems.

B. Method Comparison

To further explore the benefit of the spatial-temporal structure of AMCNN-DGCN, six widely used competitive EEG models were chosen for comparison. We reproduced these models following their settings described in the original literature. Brief introductions to these models are described in the following. More details can be referred to [11] and [24]–[27].

PSD-SVM [24]: An SVM classifier is adopted to determine the fatigue level, which is with PSD features from five frequency bands as inputs.

DE-SVM: It replaces the inputs features of PSD-SVM [24] into DE features.

CNN-A [11]: A novel channelwise CNN with a five-layer is developed to evaluate fatigue states on the preprocessed EEG data.

CNN-B [25]: A four-layer CNN is proposed for motor imagery brain-computer interface system with the preprocessed EEG signals as input.

ShallowConvNet [26]: A Shallow ConvNet for brain-computer interfaces with the preprocessed EEG signals as input.

EEGNet [27]: A compact CNN for brain-computer interfaces with the preprocessed EEG data as input.

We report the average accuracy, sensitivity, specificity, average AUC value, and ROC curve of each method in Fig. 5. We discover that AMCNN-DGCN achieved the highest accuracy among all seven methods, followed by EEGNet (94.70%) and ShallowConvNet (94.00%), respectively. The three best models are all spatiotemporal models. In addition, two hand-crafted feature-based methods, i.e., PSD-SVM and DE-SVM, cannot achieve satisfactory results due to the neglect of the spatial information of EEG signals. CNN-based models are suboptimal because flattening the EEG channels distributed on the 3-D irregular grid to a 2-D representation with a regular grid cannot adequately and accurately reflect the spatial relationship of the signal. In contrast, AMCNN-DGCN adopts the dynamically learned adjacency matrix to characterize the spatial relationship of the signal accurately, and thereby, the performance can be improved. Besides, the sensitivity and specificity of AMCNN-DGCN are 95.61% and 95.69%, respectively, which shows that AMCNN-DGCN has nearly the same classification ability to classify each state (i.e., alert state and fatigue state). The classification ability for each state can also be reflected by the average AUC value and the ROC curve. For AUC value, AMCNN-DGCN outperforms the other six EEG models (i.e., PSD-SVM, DE-SVM, CNN-A, CNN-B, Shallow ConvNet, and EEGNet) by 4.8%, 3.2%,

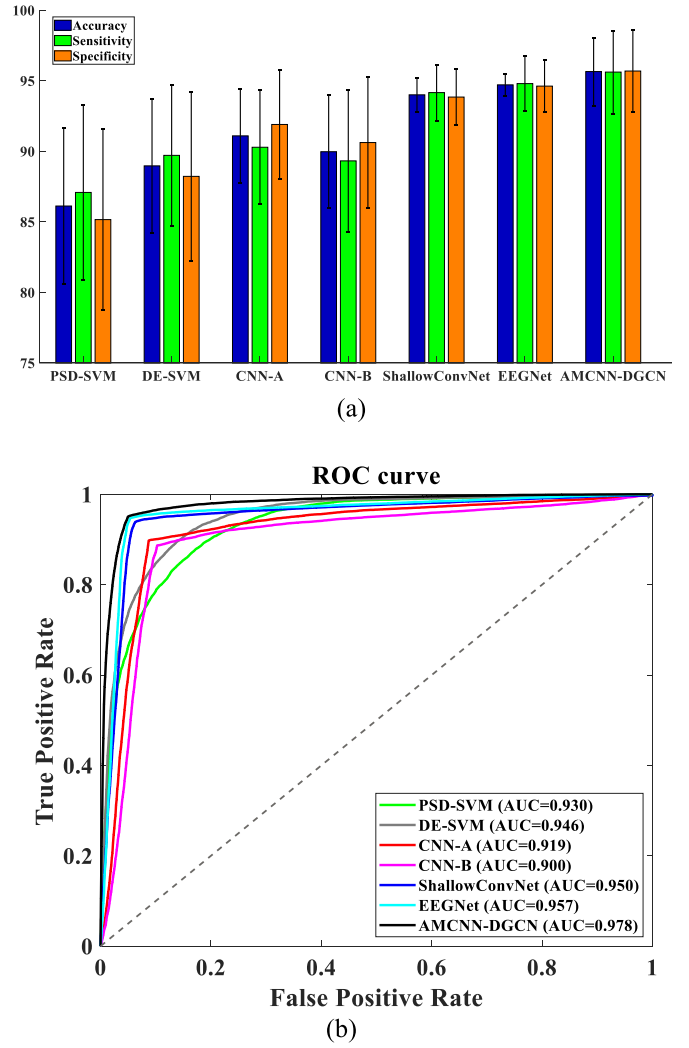


Fig. 5. (a) Comparison of Accuracy, sensitivity, and specificity for different methods. (b) Comparison of AUC value and ROC curve for different methods.

5.9%, 7.8%, 2.8%, and 2.1%, respectively. From the above-mentioned different perspectives, a conclusion can be drawn that AMCNN-DGCN has good classification performance and robustness.

C. Ablation Studies

We conducted ablation studies to assess the impact of every component of our AMCNN-DGCN model. To measure the impact of the temporal convolution block, we, respectively, replace the features (denoted as $F^{(J)}$ in Fig. 1) extracted from temporal convolution blocks to the PSD feature and DE feature, which are the widely used handcrafted features for driving fatigue detection. The generated methods are denoted by PSD-DGCN and DE-DGCN in Fig. 6, respectively. We observe in Fig. 6 that the proposed AMCNN-DGCN model significantly outperforms the PSD-DGCN and DE-DGCN by 9.82% and 6.61%, respectively. The reason is that PSD-DGCN and DE-DGCN cannot be trained end-to-end, which tends to lose some important information and, thus, yield unsatisfactory performance.

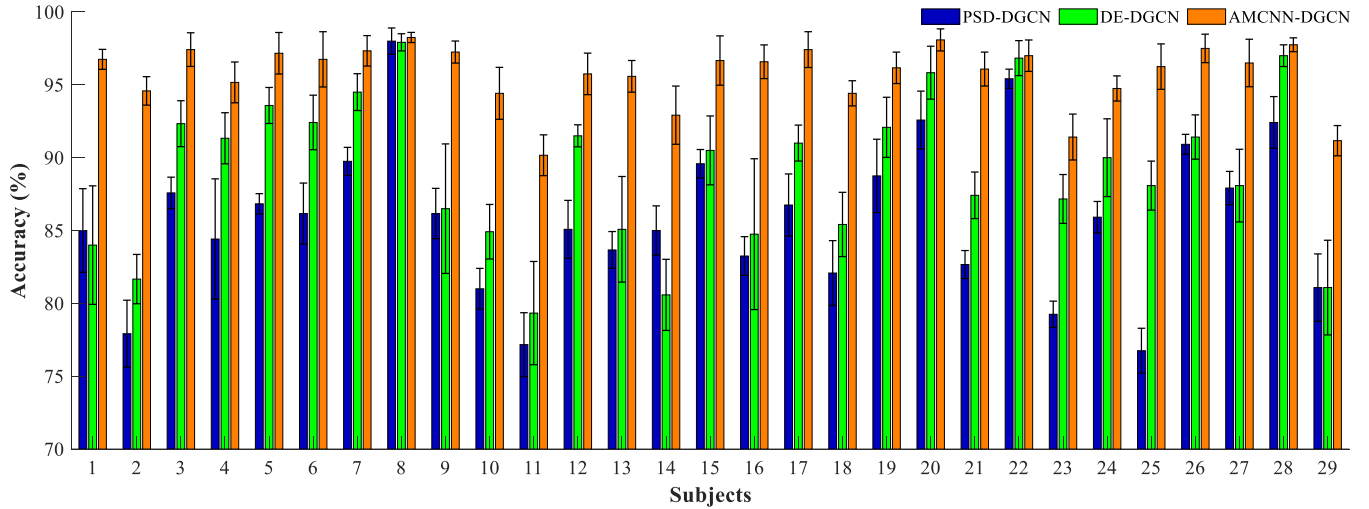


Fig. 6. Impact of the temporal convolutional block (AMCNN).

TABLE II

CLASSIFICATION ACCURACY WITH DIFFERENT ADJACENCY MATRICES

| Type of adjacency matrix | Accuracy |
|--|------------|
| Statically predetermined adjacency matrix (with random symmetric matrix) | 90.88±5.22 |
| Statically predetermined adjacency matrix (with PLI matrix) | 93.87±2.96 |
| Dynamically Learned adjacency matrix (initialized by random symmetric matrix) | 95.65±2.10 |
| Dynamically Learned adjacency matrix (initialized by PLI matrix) | 95.84±2.07 |

To measure the impact of the adjacency matrix in graph convolutional block, we compare four types of adjacency matrix in Table II. For the statically predetermined adjacency matrix, the performance of the PLI matrix significantly outperforms the random symmetric matrix. The reason is that PLI quantifies the phase synchronization between electrode signals and, thus, can represent the relationship between different EEG channels. On the contrary, the random symmetric matrix ignores the correlation of EEG channels.

Notably, the dynamically learned adjacency matrix is superior to the statically predetermined adjacency matrix, which indicates that the dynamically learned adjacency matrix is more conducive to capture the intrinsic connections of channels and, thus, helps improve the discriminability of the model. Besides, the performance of the AMCNN-DGCN model is insensitive to the initialization of the adjacency matrix, which shows that the AMCNN-DGCN model is very easy to train and implement.

D. Study of Critical Brain Regions and Connection

We employ Degree Centrality to identify the critical brain regions for driving fatigue detection. Degree Centrality is commonly used to access the importance of the nodes in the graph, measuring the connectivity of a node to other nodes [28], [29]. In the AMCNN-DGCN model, the dynamically learned adjacency matrix \mathbf{A} represents the connections between nodes, and each EEG channel is considered as a node of the graph. With the adjacency matrix \mathbf{A} , the degree of

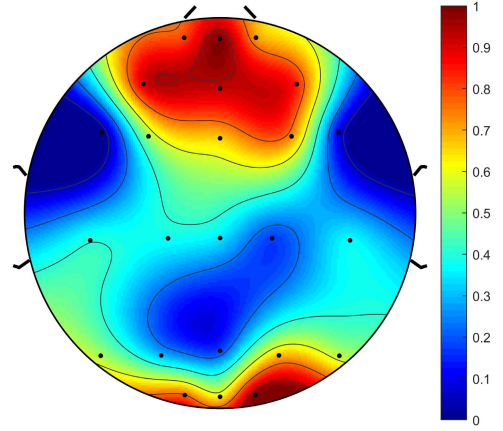


Fig. 7. Topographic maps learned from the AMCNN-DGCN model.

centrality C_i of the i th EEG electrode can be obtained by

$$C_i = \sum_{n=1}^{24} \mathbf{A}_{i,n} + \sum_{m=1}^{24} \mathbf{A}_{m,i} - 2\mathbf{A}_{i,i} \quad (i = 1, \dots, 24). \quad (6)$$

We scale the value of C to the interval of $[0, 1]$ for better visualization. From Fig. 7, we observed strong activation in the frontal and occipital regions, revealing that these regions may be closely associated with mental fatigue in the brain. Our observations are consistent with various existing studies that have suggested the frontal and occipital regions are strongly related to mental fatigue [8], [21]. More specifically, neuroscience research has revealed that the frontal lobe is responsible for the sustained attention task [30]. In addition, the occipital lobe is related to visual tasks [31]. While driving, the driver needs to observe the driving situation, which is a continuous visual task.

We also identify the critical connections for driving fatigue detection, as shown in Fig. 8. For better illustration, only the top-60 connections (about 10% of the total connections) are preserved, which is associated with the 60 largest edge weights in the learned adjacency matrix \mathbf{A} . We scale the value of the top-60 connections to the interval of $[0.2, 1]$ for better visualization. From Fig. 8, we observe that the frontal-frontal and

TABLE III
COMPARISON WITH SOME STATE-OF-THE-ART METHODS

| Author | Method | EEG channels | Subject number | Accuracy |
|-----------------------|--|--------------|----------------|----------|
| Zeng et al. 2018[33] | CNN with recent deep residual learning | 16 | 10 | 84.38% |
| Cheng et al. 2018[34] | CNN with Image-based EEG | 32 | 37 | 71.16% |
| Chai et al. 2017[35] | Sparse Deep belief networks | 32 | 43 | 90.6% |
| Gao et al. 2019[12] | Spatial-temporal CNN | 40 | 8 | 97.37% |
| Ma et al. 2019[36] | PCANet with SVM | 32 | 6 | 95% |
| Gao et al. 2019[37] | Recurrent network-based CNN | 40 | 10 | 92.95% |
| Ours | AMCNN-DGCN | 24 | 29 | 95.65% |

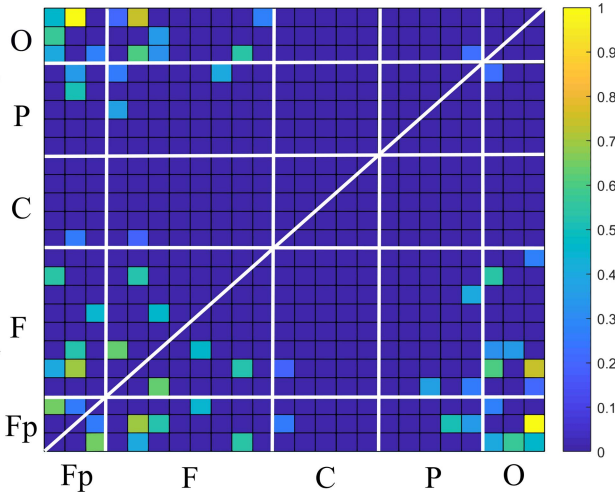


Fig. 8. Top-60 connections (about 10% of the total connections) between channels learned from AMCNN-DGCN model. Fp: frontal pole region; F: frontal region; P: parietal region; C: central region; and O: occipital region.

frontal–occipital are the strongest connections, again reflecting that the frontal and occipital regions are of great significance for driving fatigue detection.

E. Comparison With Some State-of-the-Art Methods

Table III summarizes some latest driving fatigue detection methods with EEG signals [12], [32]–[37]. Under comparable accuracy, the benefits of the proposed AMCNN-DGCN are as follows.

- 1) AMCNN-DGCN is trained with a relatively small number of EEG channels, which shows more convenient and comfortable for driving fatigue detection.
- 2) AMCNN-DGCN is validated on a relatively large number of subjects with detailed ablation studies, which demonstrates that the proposed model has a better reproducibility.

V. CONCLUSION

In this article, we proposed a unified end to end model for driving fatigue detection, called AMCNN-DGCN, to automatically capture highly discriminative features from the raw EEG data and model the intrinsic interchannel relations between different EEG channels. Experimental results verify the following conclusions.

- 1) We first introduce attention-based multiscale temporal convolutions to automatically and adaptively extract the salient pattern from the EEG data. With this elaborate

design, AMCNN-DGCN can not only overcome the tedious and time-consuming process of manual feature extraction and parameter tunings but also significantly improve classification performance. Compared with PSD-DGCN and DE-DGCN, the test accuracy is improved by up to 9.82% and 6.61%, respectively.

- 2) Compared with previous studies that trained GCN with a fixed and predetermined graph, the AMCNN-DGCN model can obtain the optimal graph connections in a data-driven way. Therefore, better performance can be obtained in AMCNN-DGCN. Compared with GCN trained with a fixed random symmetric matrix and a fixed PLI matrix, the test accuracy of AMCNN-DGCN is improved by 4.77% and 1.78%, respectively.
- 3) AMCNN-DGCN is with the temporal–spatial structure to extract more discriminative features and with the compact model to alleviate overfitting problems. For test accuracy, AMCNN-DGCN outperforms the six widely used competitive EEG models (i.e., PSD-SVM, DE-SVM, CNN-A, CNN-B, ShallowConvNet, and EEGNet) by 9.53%, 6.68%, 4.56%, 5.68%, 1.65%, and 0.94%, respectively.

In a nutshell, AMCNN-DGCN is an effective model for driving fatigue detection in many aspects. However, the design of 24 EEG electrode placements may still be inconvenient for driving fatigue detection. In the future, we will train the AMCNN-DGCN model with a considerably lower number of EEG channels that can be easily embedded in a headset. On the other hand, the hardware implementation of the AMCNN-DGCN model in the FPGA platform may further promote real-world applications of driving fatigue detection. We also leave this for future research.

REFERENCES

- [1] P. S. Rau, “Drowsy driver detection and warning system for commercial vehicle drivers: Field operational test design, data analyses, and progress,” in *Proc. 19th Int. Conf. Enhanced Saf. Vehicles*, 2005, pp. 6–9.
- [2] G. N. Dimitrakopoulos *et al.*, “Functional connectivity analysis of mental fatigue reveals different network topological alterations between driving and vigilance tasks,” *IEEE Trans. Neural Syst. Rehabil. Eng.*, vol. 26, no. 4, pp. 740–749, Apr. 2018.
- [3] P. Qi *et al.*, “Neural mechanisms of mental fatigue revisited: New insights from the brain connectome,” *Engineering*, vol. 5, no. 2, pp. 276–286, Apr. 2019.
- [4] R. Bose, H. Wang, A. Dragomir, N. Thakor, A. Bezerianos, and J. Li, “Regression-based continuous driving fatigue estimation: Toward practical implementation,” *IEEE Trans. Cogn. Developmental Syst.*, vol. 12, no. 2, pp. 323–331, Jun. 2020.
- [5] N. Gurudath and H. B. Riley, “Drowsy driving detection by EEG analysis using wavelet transform and K-means clustering,” *Procedia Comput. Sci.*, vol. 34, pp. 400–409, 2014.
- [6] Y. Xiong, J. Gao, Y. Yang, X. Yu, and W. Huang, “Classifying driving fatigue based on combined entropy measure using EEG signals,” *Int. J. Control Autom.*, vol. 9, no. 3, pp. 329–338, Mar. 2016.

- [7] F. Wang, H. Wang, and R. Fu, "Real-time ECG-based detection of fatigue driving using sample entropy," *Entropy*, vol. 20, no. 3, p. 196, Mar. 2018.
- [8] H. Wang *et al.*, "Driving fatigue recognition with functional connectivity based on phase synchronization," *IEEE Trans. Cognit. Develop. Syst.*, early access, Apr. 13, 2020, doi: [10.1109/TCDS.2020.2985539](https://doi.org/10.1109/TCDS.2020.2985539).
- [9] P. Li *et al.*, "EEG based emotion recognition by combining functional connectivity network and local activations," *IEEE Trans. Biomed. Eng.*, vol. 66, no. 10, pp. 2869–2881, Oct. 2019.
- [10] A. Omidvarnia, M. Mesbah, J. M. O'Toole, P. Colditz, and B. Boashash, "Analysis of the time-varying cortical neural connectivity in the newborn EEG: A time-frequency approach," in *Proc. Int. Workshop Syst., Signal Process. Their Appl., WOSSPA*, May 2011, pp. 179–182.
- [11] M. Hajinoroozi, Z. Mao, T.-P. Jung, C.-T. Lin, and Y. Huang, "EEG-based prediction of driver's cognitive performance by deep convolutional neural network," *Signal Process., Image Commun.*, vol. 47, pp. 549–555, Sep. 2016.
- [12] Z. Gao *et al.*, "EEG-based spatio-temporal convolutional neural network for driver fatigue evaluation," *IEEE Trans. Neural Netw. Learn. Syst.*, vol. 30, no. 9, pp. 2755–2763, Sep. 2019.
- [13] Z. Mu, J. Hu, and J. Min, "Driver fatigue detection system using electroencephalography signals based on combined entropy features," *Appl. Sci.*, vol. 7, no. 2, p. 150, Feb. 2017.
- [14] Y. Yang, Z. Gao, Y. Li, Q. Cai, N. Marwan, and J. Kurths, "A complex network-based broad learning system for detecting driver fatigue from EEG signals," *IEEE Trans. Syst., Man, Cybern. Syst.*, early access, Dec. 6, 2019, doi: [10.1109/TSMC.2019.2956022](https://doi.org/10.1109/TSMC.2019.2956022).
- [15] M. Defferrard, X. Bresson, and P. Vandergheynst, "Convolutional neural networks on graphs with fast localized spectral filtering," in *Proc. Adv. Neural Inf. Process. Syst.*, 2016, pp. 3844–3852.
- [16] W. Zhang, F. Wang, S. Wu, Z. Xu, J. Ping, and Y. Jiang, "Partial directed coherence based graph convolutional neural networks for driving fatigue detection," *Rev. Sci. Instrum.*, vol. 91, no. 7, Jul. 2020, Art. no. 074713.
- [17] T. N. Kipf and M. Welling, "Semi-supervised classification with graph convolutional networks," 2016, *arXiv:1609.02907*. [Online]. Available: <http://arxiv.org/abs/1609.02907>
- [18] F. Wu, T. Zhang, A. Holanda de Souza, Jr., C. Fifty, T. Yu, and K. Q. Weinberger, "Simplifying graph convolutional networks," 2019, *arXiv:1902.07153*. [Online]. Available: <http://arxiv.org/abs/1902.07153>
- [19] K. Xu, W. Hu, J. Leskovec, and S. Jegelka, "How powerful are graph neural networks?" 2018, *arXiv:1810.00826*. [Online]. Available: <http://arxiv.org/abs/1810.00826>
- [20] D. P. Kingma and J. Ba, "Adam: A method for stochastic optimization," 2014, *arXiv:1412.6980*. [Online]. Available: <http://arxiv.org/abs/1412.6980>
- [21] H. Wang *et al.*, "Dynamic reorganization of functional connectivity unmasks fatigue related performance declines in simulated driving," *IEEE Trans. Neural Syst. Rehabil. Eng.*, vol. 28, no. 8, pp. 1790–1799, Aug. 2020.
- [22] C. J. James and C. W. Hesse, "Independent component analysis for biomedical signals," *Physiol. Meas.*, vol. 26, no. 1, pp. R15–R39, Feb. 2005.
- [23] A. Delorme and S. Makeig, "EEGLAB: An open source toolbox for analysis of single-trial EEG dynamics including independent component analysis," *J. Neurosci. Methods*, vol. 134, no. 1, pp. 9–21, Mar. 2004.
- [24] S. Barua, M. U. Ahmed, C. Ahlström, and S. Begum, "Automatic driver sleepiness detection using EEG, EOG and contextual information," *Expert Syst. Appl.*, vol. 115, pp. 121–135, Jan. 2019.
- [25] H. Dose, J. S. Möller, H. K. Iversen, and S. Puthusserpady, "An end-to-end deep learning approach to MI-EEG signal classification for BCIs," *Expert Syst. Appl.*, vol. 114, pp. 532–542, Dec. 2018.
- [26] R. T. Schirrmeister *et al.*, "Deep learning with convolutional neural networks for EEG decoding and visualization," *Hum. Brain Mapping*, vol. 38, no. 11, pp. 5391–5420, Nov. 2017.
- [27] V. J. Lawhern, A. J. Solon, N. R. Waytowich, S. M. Gordon, C. P. Hung, and B. J. Lance, "EEGNet: A compact convolutional neural network for EEG-based brain-computer interfaces," *J. Neural Eng.*, vol. 15, no. 5, 2018, Art. no. 056013.
- [28] X. Zhang, G. Cheng, and Y. Qu, "Ontology summarization based on RDF sentence graph," in *Proc. 16th Int. Conf. World Wide Web (WWW)*, 2007, pp. 707–716.
- [29] T. Song, S. Liu, W. Zheng, Y. Zong, and Z. Cui, "Instance-adaptive graph for EEG emotion recognition," in *Proc. AAAI*, 2020, pp. 2701–2708.
- [30] N. U. F. Dosenbach *et al.*, "Distinct brain networks for adaptive and stable task control in humans," *Proc. Nat. Acad. Sci. USA*, vol. 104, no. 26, pp. 11073–11078, Jun. 2007.
- [31] X. Fan, Q. Zhou, Z. Liu, and F. Xie, "Electroencephalogram assessment of mental fatigue in visual search," *Bio-Medical Mater. Eng.*, vol. 26, no. s1, pp. S1455–S1463, Aug. 2015.
- [32] L.-H. Du, W. Liu, W.-L. Zheng, and B.-L. Lu, "Detecting driving fatigue with multimodal deep learning," in *Proc. 8th Int. IEEE/EMBS Conf. Neural Eng. (NER)*, May 2017, pp. 74–77.
- [33] H. Zeng, C. Yang, G. Dai, F. Qin, J. Zhang, and W. Kong, "EEG classification of driver mental states by deep learning," *Cognit. Neurodynamics*, vol. 12, no. 6, pp. 597–606, Dec. 2018.
- [34] E. J. Cheng, K.-Y. Young, and C.-T. Lin, "Image-based EEG signal processing for driving fatigue prediction," in *Proc. Int. Autom. Control Conf. (CACS)*, Nov. 2018, pp. 1–5.
- [35] R. Chai *et al.*, "Improving EEG-based driver fatigue classification using sparse-deep belief networks," *Frontiers Neurosci.*, vol. 11, p. 103, Mar. 2017.
- [36] Y. Ma *et al.*, "Driving fatigue detection from EEG using a modified PCANet method," *Comput. Intell. Neurosci.*, vol. 2019, Jul. 2019, Art. no. 4721863.
- [37] Z.-K. Gao, Y.-L. Li, Y.-X. Yang, and C. Ma, "A recurrence network-based convolutional neural network for fatigue driving detection from EEG," *Chaos: Interdiscipl. J. Nonlinear Sci.*, vol. 29, no. 11, Nov. 2019, Art. no. 113126.



Hongtao Wang (Member, IEEE) received the Ph.D. degree in pattern recognition and intelligent systems from the South China University of Technology, Guangzhou, China, in 2015.

He was a Visiting Research Fellow with the National University of Singapore, Singapore. He is currently a Full Professor with the Faculty of Intelligent Manufacturing and the Deputy Director of Discipline and Science & Technology Development Center, Wuyi University, Jiangmen, China, where he is also the Director of the Jiangmen Brain-like Computation and Hybrid Intelligence Research Center. His current research interests include the fields of brain-like computation, pattern recognition, deep learning, and hybrid intelligence.



Linfeng Xu was born in Guangdong, China, in 1994. He received the bachelor's degree from the Guangdong University of Petrochemical Technology, Maoming, China, in 2017. He is currently pursuing the master's degree with the Faculty of Intelligent Manufacturing, Wuyi University, Jiangmen, China.

From 2017 to 2019, he was involved in algorithm research and development in Shenzhen, China. His research interests include pattern recognition and brain-like computation.



Anastasios Bezerianos (Senior Member, IEEE) received the bachelor's degree in physics from the University of Patras, Patras, Greece, in 1975, the master's degree in telecommunications from Athens University, Athens, Greece, in 1981, and the Ph.D. degree in bioengineering from the University of Patras, Patras, Greece, in 1987.

He is currently the Head of the Cognitive Engineering (COGEN) Laboratory, N.I Health Institute, National University of Singapore, Singapore, a Professor with the NUS Graduate School for Integrative Sciences and Engineering, and a Visiting Professor with the Computer Science Department, New South Wales University (NSWU), Canberra, ACT, Australia. He has been a Professor of medical physics with the Medical School, University of Patras, since 2004. He is the Founder and the Chairman of the Biannual International Summer School on Emerging Technologies in Biomedicine, Singapore. His work is summarized in 140 journals and 217 conference proceedings publications, one book, and two patents. He has research collaborations with research institutes and universities in Japan, China, and Europe. His research entails diverse areas spanning from artificial intelligence and robotics to biomedical signal processing and brain imaging, as well as mathematical biology and systems medicine, and bioinformatics.

Dr. Bezerianos is a fellow of the European Alliance for Medical and Biological Engineering and Science (EAMBES). He is also an Associate Editor of the IEEE TRANSACTIONS ON NEURAL SYSTEMS AND REHABILITATION ENGINEERING (TNSRE), the *PLOS ONE*, and *Neuroscience Journal* and a reviewer of several international scientific journals. He is also a Registered Expert of the Horizon 2020 Program of the European Union and a reviewer of research grant proposals in Greece, Italy, Cyprus, and Canada.



Chuangquan Chen (Member, IEEE) received the Ph.D. degree in computer science from the University of Macau, Macau, in 2020.

He subsequently joined Wuyi University, Jiangmen, China, as a Distinguished Professor. His current research interests include machine learning methods and intelligent systems.



Zhiguo Zhang (Member, IEEE) received the B.Sc. degree from Tianjin University, Tianjin, China, in 2000, the M.Eng. degree from the University of Science and Technology of China, Hefei, China, in 2003, and the Ph.D. degree from the Department of Electrical and Electronic Engineering, The University of Hong Kong, Hong Kong, in 2008.

He was a Post-Doctoral Research Fellow and then a Research Assistant Professor with The University of Hong Kong from 2008 to 2014. He was an Assistant Professor with Nanyang Technological University, Singapore, in 2015, and a Professor with Sun Yat-sen University, Guangzhou, China, in 2016. He is currently a Professor with Shenzhen University, Shenzhen, China. His research interests include neural signal processing, neuroinformatics, and neural engineering.